

# Challenges of Biomolecular Detection at the Nanoscale: Nanopores and Microelectrodes

Klaus Mathwig,<sup>†,‡</sup> Tim Albrecht,<sup>‡,‡</sup> Edgar D. Goluch,<sup>§</sup> and Liza Rassaei<sup>\*,¶</sup>

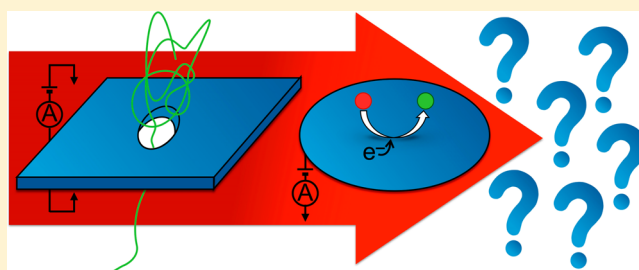
<sup>†</sup>Pharmaceutical Analysis, Groningen Research Institute of Pharmacy, University of Groningen, P.O. Box 196, 9700 AD Groningen, The Netherlands

<sup>‡</sup>Department of Chemistry, Imperial College London, Exhibition Road, South Kensington Campus, London, SW7 2AZ, U.K.

<sup>§</sup>Department of Chemical Engineering, Northeastern University, 360 Huntington Avenue, 313SN, Boston, Massachusetts 02115, United States

<sup>¶</sup>Department of Chemical Engineering, Delft University of Technology, Julianalaan 136, 2628 BL Delft, The Netherlands

**ABSTRACT:** The interest in analytical devices, which typically rely on the reactivity of a biological component for specificity, is growing rapidly. In this Perspective, we highlight current challenges in all-electrical biosensing as these systems shrink toward the nanoscale and enable the detection of analytes at the single-molecule level. We focus on two sensing principles: nanopores and amperometric microelectrode devices.



Considerable research interest toward miniaturization of analytical systems stems from the demand for more sensitive measurements for field and point-of-care practice. Miniaturization of analytical devices offers the prospect of integration of multiple steps in complex analytical procedures into a single portable device. Such devices will enable unskilled end-users to perform highly complex clinical or environmental tests, which are now only viable in large specialized central laboratories. A share of this progress is directed toward shrinking the size of detection elements to the nanoscale as well as integrating them with electronics.

Nanoscale sensors are not only desirable for point-of-care use, but they can also yield valuable molecular information in fundamental studies when a single-molecule detection level is approached. Here, molecular heterogeneities, subpopulations, intramolecular dynamics, and unsynchronized reactions, which are masked, averaged out, or otherwise invisible in ensemble measurements, can also be revealed. For example, enzyme molecules with identical primary sequences exhibit slight differences in conformation and turnover rate. This can be due to random errors that occur in the transcription and translation processes or due to the unpredictable events during the folding process.

From a sensor application standpoint, single-molecule resolution is the fundamental limit for detection as this sensitivity allows the measurement of very low-concentration assays relevant for, e.g., early stage detection of disease biomarkers.

Since the first single-molecule experiment by Rotman in 1961,<sup>1</sup> who detected the fluorescence response of individual single enzyme molecules encapsulated in microdroplets, single-molecule techniques such as optical methods, force microscopy,

and electrical methods have been developed with an exponential increase. From a practical real-world point of view, electrical methods have the advantage of facile miniaturization, ease of integration with CMOS systems, straightforward signal transduction, and lower cost. The advancement of electrical single-molecule detection systems has mostly been focused on the passage of single molecules through a single ion channel or nanopore by measuring the change in conductance of the electrolyte media. However, other electrical single molecule detections schemes have attracted attention. For example, single molecules can be detected and their dynamics can be monitored when the biomolecule of interest is attached to a field effect transistor (FET) consisting of a carbon nanotube.<sup>2–4</sup> Here, the signal is amplified by electrostatic gating of the charged functional groups of biomolecules on the surface of the underlying FET.

Several reports have already highlighted the importance of biosensing and its implications on our lives.<sup>5–8</sup> In this Perspective, we exemplify two electrical sensing principles for low numbers of molecules and the inherent challenges for molecular biodetection: nanopores, already very powerful single molecule tools, and microelectrodes (especially, microfabricated devices based on direct electron transfer). Adopting amperometric sensing, microelectrode devices are promising to achieve single-molecule biodetection for fundamental studies as well as for point-of-care applications.

**Received:** March 27, 2015

**Accepted:** April 30, 2015

**Published:** April 30, 2015

## ■ BIOSENSING AT NANOPORES

Nanopore sensors consist of a highly insulating membrane, usually with a single nanometer-sized pore, incorporated into an electrolyte-filled cell. “Biological” nanopore sensors contain a pore-forming protein, such as  $\alpha$ -hemolysin, embedded in a lipid-bilayer membrane. Here, we focus on solid-state devices, which feature a highly insulating dielectric membrane material (e.g.,  $\text{Si}_3\text{N}_4$ ,  $\text{SiO}_2$ , more recently also single-layer graphene and  $\text{MoS}_2$ ) and a pore milled with a focused electron or ion beam.<sup>9–13</sup> Hybrid devices have also been fabricated, for example, by integrating  $\alpha$ -hemolysin directly into a solid-state membrane or by designing nanopore channels from DNA Origami.<sup>14,15</sup> The fundamental working principle is the same and illustrated in Figure 1. An external electric field or other

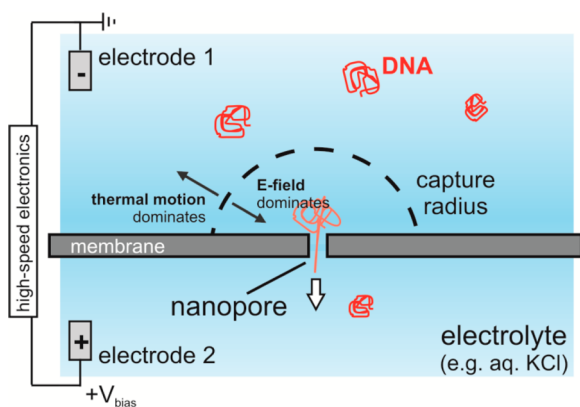


Figure 1. Basic design and working principle of a nanopore sensor. A highly insulating membrane separates two electrolyte-filled compartments, and only a nanometer-sized opening in the membrane (the “nanopore”) allows for the transport of liquid, ions, and analytes between the two reservoirs. The two electrodes are used to apply an electric field and measure the ion current through the cell. If the solution or “access” resistance is small compared to the pore resistance,  $R_{\text{acc}} \ll R_{\text{pore}}$ , the electric field at the pore is  $E \approx V_{\text{bias}}/L$ , where  $L$  is the membrane thickness. The bulk solution is then effectively field-free and DNA motion is governed by Brownian diffusion. The capture radius characterizes the distance from the pore entrance where electrophoresis becomes effective in transporting DNA. Electro-osmosis occurs when the pore walls are charged and affects the speed of DNA translocation. In the case of proteins, it may even determine the direction of transport, namely, against the electrophoretic force.<sup>19</sup>

driving force is used to drive large biopolymers, such as single- or double-stranded DNA, through the pore. Such a “translocation event” may be detected optically (fluorescence or surface-enhanced (resonance) Raman), via local probes or by measuring the ion current, if the passing polymer alters the (ionic) conductance of the nanopore (which is usually the case).<sup>16–18</sup> Features of the measured signal, such as the duration of the event, the magnitude of the signal modulation, and potential substructure, reflect the physical properties of the analyte, e.g., the length of the polymer, its relative charge, and conformation.<sup>9,10,13</sup>

The pore can be made small enough so that the analyte (say DNA) is forced into a linear conformation during translocation. In principle, this interesting and rather unique feature gives access to the individual bases (or base pairs) and may allow for compositional analysis with high spatial resolution along the DNA, at the single-molecule level. Hence, the idea of fast and

label-free DNA (or RNA) sequencing has been a major driving force in the field (and been achieved using biological pores),<sup>20,21,22</sup> even though there is also considerable interest in other applications, such as the detection of proteins and protein complexes, fragment sizing, barcoding, and gene profiling.<sup>23,24</sup> In this context, solid-state nanopore devices offer an advantage over biological channels, in that the pore size can be adapted to the analyte in question; they could be seen as a more flexible platform for biomolecular analysis.

However, several challenges inherent to (solid-state) nanopore sensing have so far prevented it from becoming a mainstream tool in biomolecular analysis and diagnostics. Rather than sequencing, which has been discussed elsewhere recently,<sup>25,26</sup> we take as an example the detection and analysis of protein/DNA complexes, e.g., for methylation profiling or DNA damage detection. It should be noted that similar considerations however apply to other applications. In these cases, the presence and relative location of proteins bound along the DNA is of interest, as illustrated in Figure 2.

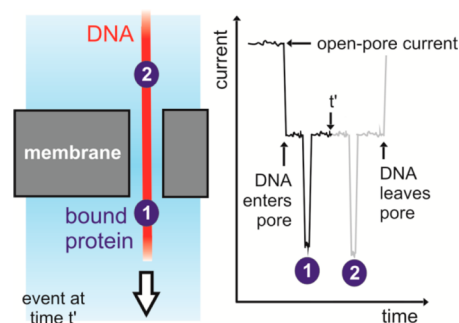


Figure 2. (Left) Illustration of a DNA/protein complex, translocating through a nanopore. (Right) Current–time trace covering the entire translocation process from DNA entry to it leaving the pore. When the DNA enters, the measured current begins to deviate from the open-pore current and remains at a certain, “DNA only” level, until the first bound protein enters the channel. The current remains at a new level until protein 1 exits, after which the “DNA only” current is re-established.  $t'$  is the moment in time shown on the left, namely, after protein 1 has left but before protein 2 has entered the pore. Analytical information may be extracted from the number of current “dips” during each event (= number of proteins bound), the time difference between each protein signal, and the start of the translocation event (related to the position on the DNA, provided the translocation speed is known) and also from the magnitude of the current change (relative size of the protein).

**Device Design.** The optimal design of solid-state nanopore sensors is at the heart of their performance, and both aspects are usually strongly coupled. The dimensions of the analyte mainly dictates the pore diameter; sub-5 nm pores allow single- and double-stranded DNA to pass through but not antibodies, which are typically around 10 nm in diameter. To a first approximation, the larger the pore volume excluded by the analyte during translocation, the larger the concomitant current change, relative to the open-pore current (surface charge effects are, however, important<sup>27</sup>). Hence, thinner membranes should be advantageous from this perspective as they allow for higher spatial resolution. On the other hand, a thinner membrane may also increase the device capacitance, thus increasing the (capacitive) noise and decreasing the time resolution of the sensor.<sup>28</sup> As a compromise, the membrane could be thin in the probe region (i.e., inside the pore) but thick and well-insulated

from the solution everywhere else.<sup>29</sup> Alas, a thinner membrane usually means that the local electric field is higher, increasing the speed of translocation and the time resolution required for reliable detection. Higher local electric fields may also render the pore unstable, by inducing local (electro-)chemical reactions and decrease the lifetime of the device.<sup>30,31</sup>

**Translocation Speed and Time Resolution.** If a 10 kbp ( $\sim 3.4 \mu\text{m}$ ) long, linear piece of DNA with a single bound antibody (diameter  $\sim 10 \text{ nm}$ ) translocates in  $\sim 1 \text{ ms}$  through a pore channel of  $L = 50 \text{ nm}$ , then the bound antibody spends only about  $3 \mu\text{s}$  in the sensing region. With electric current modulations usually in the region of hundreds of picoamps, the time resolution required to reliably detect the event represents a significant challenge. Optimizing the electronics design and decreasing device capacitance to well below  $10 \text{ pF}$  by miniaturization, as well as replacing “lossy” materials such as Si, has brought significant improvements in this regard, and the detection of even very short single-stranded DNA at low microsecond time resolution has indeed been achieved.<sup>32–35</sup> In addition, replacing KCl with LiCl or NaCl as the electrolyte has, perhaps at first glance unexpectedly, lead to a slowing down of DNA translocation, presumably due to a change in the DNA charge.<sup>36</sup>

**Fluctuations.** Determining the position of a bound protein or label on the DNA would require knowledge of the translocation speed or, at least, that the latter remains constant. If that is not the case, the measurement is affected by an unknown error. While electrophoretic transport tends to dominate DNA motion across the pore, especially at high  $V_{\text{bias}}$ , random fluctuations are always present. The actual speed of the DNA is then a function of time and changes in a stochastic manner.<sup>37,38</sup> Adsorption of DNA-bound proteins inside the pore channel can complicate matters further and it has indeed been shown that even a single protein bound to DNA can affect the translocation dynamics significantly.<sup>39,40</sup>

**Translocation Statistics and Total Analysis Time.** The translocation characteristics of an analyte (e.g., time, current change) are best represented in terms of distributions (approximately Gaussian or stretched Gaussian), as a result of the stochastic (Brownian) nature of transport toward the pore as well as fluctuations described above. In order to extract analytically meaningful information, it is often necessary to detect and analyze several hundreds if not thousands of translocation events. Only if the “signal-to-noise ratio”, e.g., the difference between the current changes for different analytes is very large, can they be differentiated with sufficient confidence even at the single-molecule level.<sup>41</sup> Otherwise, the total analysis time may be relatively long, say around  $100 \text{ s}$  for a translocation frequency of  $10 \text{ Hz}$  and  $1000$  events. The translocation frequency may be increased to some extent by increasing the solution concentration. However, too high concentrations can lead to crowding (multiple translocations at the same time) or even pore clogging or be incompatible with the solution chemistry involved (e.g., in the context of antibody/DNA binding). In practice, high picomolar or low nanomolar concentrations are common, depending on the analyte. Binding the analyte on the surface of a lipid-bilayer coated solid-state device has been devised as an elegant way to introduce enhanced specificity and to preconcentrate analytes prior to analysis (both via the specificity and binding affinity of surface receptors).

While further aspects could be added here, the above illustrates that there is no “one size fits all” and that the actual

device design requires careful consideration of the target analyte and the context of the sensing application. The speed and sensitivity of electric detection may at some point reach its fundamental limits and slowing down the translocation process by a suitable electrolyte<sup>36</sup> or by surface modification<sup>42</sup> may then be a way forward. The integration of molecular machines or processive enzymes with a solid-state nanopore platform is an intriguing prospect in this context, since it could also help reduce fluctuations and enhance control over the polymer strand inside the pore. The translocation speed is then essentially defined by the processivity of the enzyme, which is typically in the millisecond regime and hence easier to handle from an electronic point of view. It would require robust immobilization strategies that allow the enzyme to be placed into the correct location (say, the entrance of the channel using DNA Origami<sup>43</sup>) and compatibility between enzyme and the analyte.

## ■ BIOSENSING WITH MICROELECTRODES

One of the dreams of analytical chemists is to develop sensors that can measure very low analyte concentrations or even a single analyte molecule, especially when it comes to early detection of disease biomarkers. Among all methods developed for nanoscale biosensing applications, amperometric methods are promising due to their simplicity and ease of integration with other platforms. The fundamental working principle of an amperometry sensor is the electron transfer between redox-active molecules and an electrode. In this type of platform, a biomolecule converts biological information to chemical information, which is then transduced into an electrical current signal. Here, the bias potential and the magnitude of the current directly reflect the electrochemical properties of the analyte. Thus, the operation is often much simpler than optical methods. However, several inherent challenges have so far prevented amperometric sensing from becoming a mainstream tool in studying individual single (bio)molecules. Here, we point out these challenges.

**Signal Detection.** The main challenge for the detection of low numbers of molecules at microelectrodes is the small current signal obtained from individual molecules as the sensors lack intrinsic amplification. The electrodes can be fabricated small enough so that only a few analytes exchange electrons at a time for a given concentration. However, if a single target analyte molecule is oxidized or reduced at the electrode surface, only  $n$  electrons ( $n = 1, 2, 3$  depending on the molecule oxidation state) are exchanged. This charge is far too small to be detected with state-of-the-art electrical amplifiers at ambient temperature. Ultimately, the measurable current level is required to exceed instrumental noise. The smallest detectable current (under ambient conditions and using state-of-the-art electrical amplifiers) needs to be significantly higher than  $1 \text{ fA}$  which corresponds to about  $10\,000$  electron exchanges per second.

Different approaches exist to overcome or circumvent this limitation. One way is to use enzymes, which not only contribute a single charge transfer per molecule but facilitate a continuous charge transfer by turning over substrate molecules at a high rate. Hoeben et al. employed this approach to study [NiFe]-hydrogenase enzymes immobilized on the surface of a  $70 \text{ nm} \times 70 \text{ nm}$  microfabricated gold electrode.<sup>44</sup> Upon biasing the electrode, hydrogen was oxidized, generating  $2 \text{ e}^-$  at a very high turnover rate of approximately  $1500 \text{ s}^{-1}$  to  $9000 \text{ s}^{-1}$  (see Figure 3A). While no single enzyme molecule was detected in

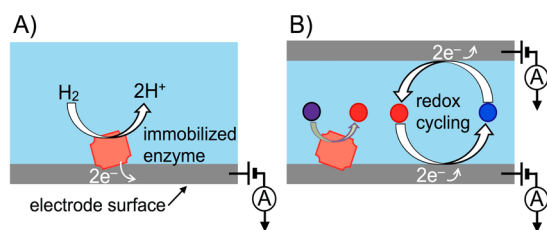


**Figure 3.** Scheme showing enzymatic biodetection by amperometric sensing at microelectrodes: (A) The enzyme [NiFe]-Hydrogenase (red), immobilized on a gold electrode, oxidizes  $\text{H}_2$  at a turnover rate of  $\sim 1500$  to  $9000 \text{ s}^{-1}$ . As each enzyme generates a corresponding current of  $\sim 0.5$  to  $3 \text{ fA}$ , it is possible to sense  $<50$  active enzymes (see ref 44). (B) The enzyme tyrosinase (red) is immobilized on the gold electrodes at the walls of a nanofluidic channel. Redox-inactive phenols (dark blue) are catalyzed into the redox-active couple catechol/quinone (red, blue), which generates a highly amplified current per product molecule by cycling in between electrodes separated by a  $200 \text{ nm}$  gap. Figure adapted from ref 45. Copyright 2014 American Chemical Society.

this study, based on the observed turnover current of  $22 \text{ fA}$ , the number of active enzymes was estimated to be  $\sim 8$  to  $46$  enzyme molecules (based on  $k_{\text{max}} = 9000 \text{ s}^{-1}$  to  $1500 \text{ s}^{-1}$ , respectively).

Another way to amplify the electrochemical signal is redox cycling between two independently biased electrodes in a nanogap configuration. Species diffuse across the gap via Brownian motion and they are oxidized (or reduced) at the first electrode. Then, they diffuse toward the second electrode where they are reduced (or oxidized) back into their original forms. Thus, for a sufficiently short diffusive path (distance between the electrodes) each molecule contributes several thousand electrons per second to the detected current. This leads to a large corresponding boost in signal.

The use of redox cycling for detection of individual single molecules was first reported in 1995.<sup>46–48</sup> Fan and Bard reported the detection of small numbers of molecules (1–10) trapped in a minuscule volume of a dilute solution of the electroactive species between a wax-shrouded Pt–Ir tip of  $\sim 10 \mu\text{m}$  and a conductive substrate using a scanning electrochemical microscope setup. Redox cycling of electroactive molecules between the tip and the substrate was shown to yield a current of  $0.7 \text{ pA/molecule}$  detected as large relative fluctuations having a step-like character as the molecules moved into and out of detection zone.

A similar configuration was reported by Sun and Mirkin where a zeptoliter volume solution was trapped in a nanogap between a disk-like recessed Pt nanoelectrode shrouded in glass and a Hg bath.<sup>49</sup> Large variations in diffusion-limited current were observed at concentrations corresponding approximately to a single-molecule occupancy in the detection zone and were attributed to different discrete numbers of redox molecules being trapped in the detection volume.

Thanks to advances in microfabrication and their accessibility and extension to other fields of science such as analytical chemistry,<sup>50,51</sup> Lemay et al. devised and fabricated an electrochemical nanofluidic sensor device<sup>52</sup> which enabled a more systematic approach to electrical single-molecule detection based on redox cycling.<sup>53,54</sup> As shown in Figure 3B, this nanogap sensor consists of two parallel microelectrodes separated by a thin film of fluid ( $<200 \text{ nm}$ ) on a chip, and the redox cycling occurs in a confined space of a nanocavity. Compared to the SECM method reported in 1995,<sup>48</sup> the new

sensor has the advantage that photolithography yields a large number of virtually identical devices with a well-determined geometry. Moreover, it allows more flexibility for future integration with CMOS systems for practical applications. In nanogap devices with a gap of  $40 \text{ nm}$ , single redox-active molecules in aqueous solution have generated currents of  $20 \text{ fA}$ .<sup>54</sup> Thus, the nanogap sensors can be employed in fundamental bioelectrochemical experiments, such as localized neurotransmitter release, or studies of single enzymes or single-cell electrochemical assays.<sup>51</sup>

As a step forward toward single-molecule bioelectrochemical detection, we recently integrated an enzymatic recognition element in a nanofluidic gap sensor so that the detection and electrochemical signal transduction occurred within a  $6 \text{ fL}$  volume.<sup>45</sup> The enzyme tyrosinase was locally immobilized via a thiol bond into a microfabricated gold nanogap electrochemical transducer. Tyrosinase catalyzes the oxidation of redox-inactive monophenols into the redox-active couple catechol/quinone at a turnover rate of  $\sim 14 \text{ s}^{-1}$ <sup>55</sup> which then undergoes redox cycling in the nanogap. The short diffusion time between the two electrodes ( $<1 \text{ ms}$  for a  $200 \text{ nm}$  gap) ensures an amplified current. Although detection at the single enzyme level was not achieved in this study, the activity of approximately  $5000$  immobilized active enzymes was studied; only  $120 \text{ zmol}$  of product molecules in the nanochannel were detected for a substrate concentration of  $25 \mu\text{M}$ . In principle, this approach can be extended to study single enzyme molecules provided that several challenges related to the enzyme immobilization and device design are overcome.

The inherent amplification of an electrocatalytic current can also be employed for the detection of individual nanoparticles.<sup>56,57</sup> Here, the catalytic process results in amplification, as a single catalyst provides a continuous stream of electron-transfer events leading to a measurable current. This approach has recently been applied successfully to nanoscale catalysts, namely, individual metal nanoparticles. In this method, the potential of the working electrode is set at a value so that little or no faradaic current flows even in the presence of a high concentration of a kinetically slow redox molecule. Upon addition of nanoparticles (which catalyze the oxidation and reduction of the redox molecules), individual current transients are observed due to the collisions of individual nanoparticles with the electrode surface and subsequent electrocatalytic reactions of the redox molecules. This method can be extended to study single biomolecules. This principle was recently employed for detection of individual DNA hybridization events (see Figure 4).<sup>58</sup> Here, a gold microband electrode was modified with a sequence of single-stranded DNA molecules, and real-time individual hybridization events of platinum

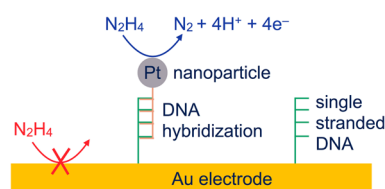


**Figure 4.** Electrochemical amplification.<sup>58</sup> Hybridization of a single DNA target and subsequent electrocatalytic oxidation of  $\text{N}_2\text{H}_4$  at the Pt nanoparticle. Figure adapted with permission from ref 58. Copyright 2013 Royal Society of Chemistry.

nanoparticle tagged DNA were monitored as current steps raised from the electrocatalytic oxidation of  $N_2H_4$ .

**Adsorption.** When micro- or nanoscale systems are employed, the role of parasitic adsorption on electrode surfaces is greatly amplified. While molecules in a biorecognition layer are most often immobilized purposely, nonspecific adsorption greatly reduces the current signal from molecules detected by redox cycling, as these should traverse a nanogap a thousand times per second by diffusing freely. In nanochannels, the surface-to-volume ratio can exceed  $10^7\text{ m}^{-1}$ , and the smallest adsorption affinities and adsorption times, which are negligible at the macro- or microscale, often lead to the effect that molecules are adsorbed most of the time. This is especially noticeable as lower numbers of molecules are measured. The first approach to minimize adsorption (and also fouling and passivation in general) is the correct selection of electrode materials. For example, it is known that redox active molecules adsorb more on noble metal electrodes such as gold or platinum compared to carbon or boron-doped diamond electrodes. Another approach is to functionalize the electrode surface with a short self-assembled monolayer with suitable end groups.<sup>59</sup> The main challenge here is to obtain a thin uniform coating to ensure fast electron transfer via this layer as the thickness of this layer affects the electron-transfer and therefore the magnitude of the signal. The adsorption of outer-sphere redox molecules is a complex process and depends on a variety of factors such as the electronic structure of the metal–solution interface, the nature of the supporting electrolyte and the adsorbate as well as electrostatic effects depending on the potential of the electrode.<sup>60</sup> Thus, better insights into the adsorption and effective methods to control it are required.<sup>61</sup>

**Biorecognition Layer.** Detection most often relies on incorporation of a biorecognition layer for hybridization, enzymatic reactions, or antigen–antibody interactions. In general, it is a challenge to achieve a reproducibly homogeneous, dense, and highly active biolayer as surface areas shrink. For single-molecule detection at a microelectrode or in a nanofluidic channel, it is even more challenging to confine the biomolecule immobilization to submicrometer dimensions. This may be achieved via the interplay of enzyme concentration and incubation time or via controlled immobilization of many enzyme molecules and deactivation of the extra enzyme molecules by an inhibitor. However, the selective immobilization of the biomolecule on the transducer continues to be a substantial challenge at the single-molecule level, as the biomolecule is also exposed to microfluidic feedthroughs and the wall of the detection channel.

**Device Design.** For any amperometric detection, a small electrode is beneficial. An electrode area smaller than the diffusion layer (approximately  $25\text{ }\mu\text{m}$  diameter) allows very efficient mass transport of analytes to the electrode surface. This allows faster electrochemical processes to be studied while parasitic double layer capacitances and ohmic losses are suppressed. Thus, the RC charging time is decreased, the response is fast, and the influence and necessity of a counter electrode and a supporting electrolyte is minimized.<sup>62</sup>

In a nanochannel device with target analytes moving freely in solution, a typical detection volume of several femtoliters is still very large when the sensors are employed for single-molecule sensing. Only at a concentration well below  $1\text{ nM}$  is one molecule at a time located on average within the detection volume. To enable single molecule studies at higher concentrations (where trace contaminations with other electro-

chemically active species are more tolerable), a greatly reduced volume is necessary. This can be achieved not only by a smaller electrode distance but also by a reduced electrode size. Miniaturization is ultimately limited by lithographic resolution (about  $1\text{ }\mu\text{m}$  if photolithography is used).

For practical applications, simultaneous selective detection of multiple analytes at low concentrations is one of the ultimate goals of analytical chemistry. Amperometric detection can offer a high selectivity, e.g., redox cycling is selective for reversible redox-active molecules over nonredox (single reduction or oxidation only) molecules, but the method still lacks selectivity for redox molecules with similar oxidation/reduction potentials. Thus, using a biorecognition layer selective to a specific substrate may solve this challenge.

## CONCLUSIONS

Technologies which provide accurate and sensitive biomolecule detection are important in the fields of medical science, biotechnology, biology, and biophysics, for practical point-of-care applications as well as for fundamental studies of single biomolecules. Nanopore sensors are already widely used tools which sense single molecules routinely.

Amperometric sensors are not yet at the stage of development to be employed as practical tools for single-molecule sensing. The main challenge to overcome is a boost in sensitivity, i.e., the signal per molecule. For all sensors, even when they are used to study ensembles of molecules, miniaturization toward the nanoscale offers a large variety of benefits, and we foresee substantial progress in this direction in the future. The most important challenge here is the definition of a reliable and reproducible biorecognition layer: it lies at the heart of the biosensor and is the first step in the detection process but difficult to implement at the nanoscale.

This important challenge of surface materials is shared with nanopore sensors, which require highly controlled surface properties to prevent fouling as well as ensuring long-term stability and operation. The further advancement of both nanopore and microelectrode sensors also depends strongly on measurement electronics which set limits to sensitivity as well as time resolution. The common challenge lies in the development of customized or integrated electronics solutions. We envision that also a combined approach of integrated nanopores/electrodes<sup>17,63</sup> might prove beneficial in future sensors.

When it comes to real-world applications, often specificity of detection of low concentrations of an analyte in a background of a complex mixture is more important than single-molecule sensitivity. We anticipate that sensors manufactured by standard microfabrication will be most successful for such applications. They will benefit from both the cost-effectiveness of massively parallel fabrication and the possibility of on-chip integration of signal processing.

## AUTHOR INFORMATION

### Corresponding Author

\*E-mail: l.rassaei@tudelft.nl.

### Author Contributions

<sup>†</sup>K.M. and T.A. contributed equally.

### Notes

The authors declare no competing financial interest.

## REFERENCES

- (1) Rotman, B. *Proc. Natl. Acad. Sci. U.S.A.* **1961**, *47*, 1981.
- (2) Choi, Y.; Olsen, T. J.; Sims, P. C.; Moody, I. S.; Corso, B. L.; Dang, M. N.; Weiss, G. A.; Collins, P. G. *Nano Lett.* **2013**, *13*, 625–631.
- (3) Besteman, K.; Lee, J.-O.; Wiertz, F. G.; Heering, H. A.; Dekker, C. *Nano Lett.* **2003**, *3*, 727–730.
- (4) Sorgenfrei, S.; Chiu, C.-y.; Gonzalez, R. L., Jr; Yu, Y.-J.; Kim, P.; Nuckolls, C.; Shepard, K. L. *Nat. Nanotechnol.* **2011**, *6*, 126–132.
- (5) Taleat, Z.; Mathwig, K.; Sudhölter, E. J.; Rassaei, L. *TrAC, Trends Anal. Chem.* **2015**, *66*, 80–89.
- (6) Kelley, S. O.; Mirkin, C. A.; Walt, D. R.; Ismagilov, R. F.; Toner, M.; Sargent, E. H. *Nat. Nanotechnol.* **2014**, *9*, 969–980.
- (7) Turner, A. P. *Chem. Soc. Rev.* **2013**, *42*, 3184–3196.
- (8) Rassaei, L.; Olthuis, W.; Tsujimura, S.; Sudhölter, E. J.; van den Berg, A. *Anal. Bioanal. Chem.* **2014**, *406*, 123–137.
- (9) Howorka, S.; Siwy, Z. *Chem. Soc. Rev.* **2009**, *38*, 2360–2384.
- (10) Ying, Y.-L.; Cao, C.; Long, Y.-T. *Analyst* **2014**, *139*, 3826–3835.
- (11) Garaj, S.; Hubbard, W.; Reina, A.; Kong, J.; Branton, D.; Golovchenko, J. *Nature* **2010**, *467*, 190–193.
- (12) Liu, K.; Feng, J.; Kis, A.; Radenovic, A. *ACS Nano* **2014**, *8*, 2504–2511.
- (13) Venkatesan, B. M.; Bashir, R. *Nat. Nanotechnol.* **2011**, *6*, 615–624.
- (14) Bell, N. A.; Keyser, U. F. *FEBS Lett.* **2014**, *588*, 3564–3570.
- (15) Hall, A. R.; Scott, A.; Rotem, D.; Mehta, K. K.; Bayley, H.; Dekker, C. *Nat. Nanotechnol.* **2010**, *5* (12), 874–877.
- (16) Chansin, G. A.; Mulero, R.; Hong, J.; Kim, M. J.; Demello, A. J.; Edel, J. B. *Nano Lett.* **2007**, *7*, 2901–2906.
- (17) Ivanov, A. P.; Instuli, E.; McGilvery, C. M.; Baldwin, G.; McComb, D. W.; Albrecht, T.; Edel, J. B. *Nano Lett.* **2010**, *11*, 279–285.
- (18) Cecchini, M. P.; Wiener, A.; Turek, V. A.; Chon, H.; Lee, S.; Ivanov, A. P.; McComb, D. W.; Choo, J.; Albrecht, T.; Maier, S. A.; Edel, J. B. *Nano Lett.* **2013**, *13*, 4602–4609.
- (19) Firmkes, M.; Pedone, D.; Knezevic, J.; Döblinger, M.; Rant, U. *Nano Lett.* **2010**, *10*, 2162–2167.
- (20) Mikheyev, A. S.; Tin, M. M. *Mol. Ecol. Resour.* **2014**, *14*, 1097–1102.
- (21) Manrao, E. A.; Derrington, I. M.; Laszlo, A. H.; Langford, K. W.; Hopper, M. K.; Gillgren, N.; Pavlenok, M.; Niederweis, M.; Gundlach, J. H. *Nat. Biotechnol.* **2012**, *30*, 349–353.
- (22) Hayden, E. C. *Nature* **2015**, *521*, 15–16.
- (23) Wei, R.; Gatterdam, V.; Wieneke, R.; Tampé, R.; Rant, U. *Nat. Nanotechnol.* **2012**, *7*, 257–263.
- (24) Japrun, D.; Dogan, J.; Freedman, K. J.; Nadzeyka, A.; Bauerdick, S.; Albrecht, T.; Kim, M. J.; Jemth, P.; Edel, J. B. *Anal. Chem.* **2013**, *85*, 2449–2456.
- (25) Carson, S.; Wanunu, M. *Nanotechnology* **2015**, *26*, 074004.
- (26) Steinbock, L.; Radenovic, A. *Nanotechnology* **2015**, *26*, 074003.
- (27) Lan, W.-J.; Kubeil, C.; Xiong, J.-W.; Bund, A.; White, H. S. *J. Phys. Chem. C* **2014**, *118*, 2726–2734.
- (28) Edel, J. B.; Albrecht, T. *Engineered Nanopores for Bioanalytical Applications*; William Andrew: Norwich, NY, 2013.
- (29) Wanunu, M.; Dadosh, T.; Ray, V.; Jin, J.; McReynolds, L.; Drndić, M. *Nat. Nanotechnol.* **2010**, *5*, 807–814.
- (30) Ayub, M.; Ivanov, A.; Instuli, E.; Cecchini, M.; Chansin, G.; McGilvery, C.; Hong, J.; Baldwin, G.; McComb, D.; Edel, J. B.; Albrecht, T. *Electrochim. Acta* **2010**, *55*, 8237–8243.
- (31) Rutkowska, A.; Freedman, K. J.; Skalkowska, J.; Kim, M.; Edel, J. B.; Albrecht, T. *Anal. Chem.* **2015**, *87*, 2337–2344.
- (32) Rosenstein, J. K.; Wanunu, M.; Merchant, C. A.; Drndić, M.; Shepard, K. L. *Nat. Methods* **2012**, *9*, 487–492.
- (33) Venta, K.; Shemer, G.; Puster, M.; Rodriguez-Manzo, J. A.; Balan, A.; Rosenstein, J. K.; Shepard, K.; Drndić, M. *ACS Nano* **2013**, *7*, 4629–4636.
- (34) Balan, A.; Machielse, B.; Niedzwiecki, D.; Lin, J.; Ong, P.; Engelke, R.; Shepard, K. L.; Drndić, M. *Nano Lett.* **2014**, *14*, 7215–7220.
- (35) Lee, M.-H.; Kumar, A.; Park, K.-B.; Cho, S.-Y.; Kim, H.-M.; Lim, M.-C.; Kim, Y.-R.; Kim, K.-B. *Sci. Rep.* **2014**, *4*, 7448.
- (36) Kowalczyk, S. W.; Wells, D. B.; Aksimentiev, A.; Dekker, C. *Nano Lett.* **2012**, *12*, 1038–1044.
- (37) Singer, A.; Wanunu, M.; Morrison, W.; Kuhn, H.; Frank-Kamenetskii, M.; Meller, A. *Nano Lett.* **2010**, *10*, 738–742.
- (38) Plesa, C.; van Loo, N.; Ketterer, P.; Dietz, H.; Dekker, C. *Nano Lett.* **2015**, *15*, 732–737.
- (39) Spiering, A.; Getfert, S.; Sischa, A.; Reimann, P.; Anselmetti, D. *Nano Lett.* **2011**, *11*, 2978–2982.
- (40) Japrun, D.; Bahrami, A.; Nadzeyka, A.; Peto, L.; Bauerdick, S.; Edel, J. B.; Albrecht, T. *J. Phys. Chem. B* **2014**, *118*, 11605–11612.
- (41) Kumar, S.; Tao, C.; Chien, M.; Hellner, B.; Balijepalli, A.; Robertson, J. W. F.; Li, Z.; Russo, J. J.; Reiner, J. E.; Kasianowicz, J. J.; Ju, J. *Sci. Rep.* **2012**, *2*, 684.
- (42) Yusko, E. C.; Johnson, J. M.; Majd, S.; Prangko, P.; Rollings, R. C.; Li, J.; Yang, J.; Mayer, M. *Nat. Nanotechnol.* **2011**, *6*, 253–260.
- (43) Bell, N. A.; Engst, C. R.; Ablay, M.; Divitini, G.; Ducati, C.; Liedl, T.; Keyser, U. F. *Nano Lett.* **2011**, *12*, 512–517.
- (44) Hoeben, F. J.; Heller, I.; Albracht, S. P.; Dekker, C.; Lemay, S. G.; Heering, H. A. *Langmuir* **2008**, *24*, 5925–5931.
- (45) Rassaei, L.; Mathwig, K.; Kang, S.; Heering, H. A.; Lemay, S. G. *ACS Nano* **2014**, *8*, 8278–8284.
- (46) Fan, F.-R. F.; Bard, A. J. *Science* **1995**, *267*, 871–874.
- (47) Fan, F.-R. F.; Kwak, J.; Bard, A. J. *J. Am. Chem. Soc.* **1996**, *118*, 9669–9675.
- (48) Bard, A. J.; Fan, F.-R. F. *Acc. Chem. Res.* **1996**, *29*, 572–578.
- (49) Sun, P.; Mirkin, M. V. *J. Am. Chem. Soc.* **2008**, *130*, 8241–8250.
- (50) Rassaei, L.; Singh, P. S.; Lemay, S. G. *Anal. Chem.* **2011**, *83*, 3974–3980.
- (51) Mathwig, K.; Aartsma, T. J.; Canters, G. W.; Lemay, S. G. *Annu. Rev. Anal. Chem.* **2014**, *7*, 383–404.
- (52) Zevenbergen, M. A. G.; Krapf, D.; Zuiddam, M. R.; Lemay, S. G. *Nano Lett.* **2007**, *7*, 384–388.
- (53) Zevenbergen, M. A.; Singh, P. S.; Goluch, E. D.; Wolfrum, B. L.; Lemay, S. G. *Nano Lett.* **2011**, *11*, 2881–2886.
- (54) Kang, S.; Nieuwenhuis, A. F.; Mathwig, K.; Mampallil, D.; Lemay, S. G. *ACS Nano* **2013**, *7*, 10931–10937.
- (55) Rassaei, L.; Cui, J.; Goluch, E. D.; Lemay, S. G. *Anal. Bioanal. Chem.* **2012**, *403*, 1577–1584.
- (56) Xiao, X.; Bard, A. J. *J. Am. Chem. Soc.* **2007**, *129*, 9610–9612.
- (57) Xiao, X.; Fan, F.-R. F.; Zhou, J.; Bard, A. J. *J. Am. Chem. Soc.* **2008**, *130*, 16669–16677.
- (58) Alligrant, T. M.; Nettleton, E. G.; Crooks, R. M. *Lab Chip* **2013**, *13*, 349–354.
- (59) Singh, P. S.; Chan, H.-S. M.; Kang, S.; Lemay, S. G. *J. Am. Chem. Soc.* **2011**, *133*, 18289–18295.
- (60) Mampallil, D.; Mathwig, K.; Kang, S.; Lemay, S. G. *J. Phys. Chem. Lett.* **2014**, *5*, 636–640.
- (61) Kätelhön, E.; Krause, K. J.; Mathwig, K.; Lemay, S. G.; Wolfrum, B. *ACS Nano* **2014**, *8*, 4924–4930.
- (62) Murray, R. W. *Chem. Rev.* **2008**, *108*, 2688–2720.
- (63) Ivanov, A. P.; Freedman, K. J.; Kim, M. J.; Albrecht, T.; Edel, J. B. *ACS Nano* **2014**, *8*, 1940–1948.